Journal of Fluorine Chemistry 132 (2011) 740–746

Contents lists available at ScienceDirect

Journal of Fluorine Chemistry

journal homepage: www.elsevier.com/locate/fluor

Jahn–Teller-distorted dimeric anions in (cat)$[Mn_2F_8(H_2O)_2]\cdot 2H_2O$ (cat = $pipzH_2$, $dabcoH_2$) and $(dabcoH_2)_2[Mn_2F_8(H_2PO_4)_2]$

Gerry Rother [b,1], Ronald Stief [a,2], Ursula Bentrup [b,3], Werner Massa [a,*]

[a] Fachbereich Chemie, Philipps-Universität, 35032 Marburg, Germany
[b] Institut für Angewandte Chemie Berlin-Adlershof e.V., 12484 Berlin, Germany

ARTICLE INFO

Article history:
Received 8 March 2011
Received in revised form 13 May 2011
Accepted 17 May 2011
Available online 26 May 2011

Dedicated to Prof. Alain Tressaud on the occasion of receiving the ACS award for creative work in fluorine chemistry.

Keywords:
Manganese(III)
Fluoromanganate(III)
Jahn–Teller effect
Crystal structure
Fluoride phosphate
Dimeric anion

ABSTRACT

Using biprotonated dabco (1,4-diazabicyclo[2.2.2]octane) or pipz (piperazine) as counter cations, mixed-ligand fluoromanganates(III) with dimeric anions could be prepared from hydrofluoric acid solutions. The crystal structures were determined by X-ray diffraction on single crystals: $dabcoH_2[Mn_2F_8(H_2O)_2]\cdot 2H_2O$ (**1**), space group $P2_1$, $Z = 2$, $a = 6.944(1)$, $b = 14.689(3)$, $c = 7.307(1)$ Å, $\beta = 93.75(3)^\circ$, $R_1 = 0.0240$; $pipzH_2[Mn_2F_8(H_2O)_2]\cdot 2H_2O$ (**2**), space group $P\bar{1}$, $Z = 2$, $a = 6.977(1)$, $b = 8.760(2)$, $c = 12.584(3)$ Å, $\alpha = 83.79(3)$, $\beta = 74.25(3)$, $\gamma = 71.20(3)^\circ$, $R_1 = 0.0451$; $(dabcoH_2)_2[Mn_2F_8(H_2PO_4)_2]$ (**3**), space group $P2_1/n$, $Z = 4$, $a = 9.3447(4)$, $b = 12.5208(4)$, $c = 9.7591(6)$ Å, $\beta = 94.392(8)^\circ$, $R_1 = 0.0280$. All three compounds show dimeric anions formed by $[MnF_5O]$ octahedra (O from oxo ligands) sharing a common edge, with strongly asymmetric double fluorine bridges. In contrast to analogous dimeric anions of Al or Fe(III), the oxo ligands (H_2O (**1**,**2**) or phosphate (**3**)) are in equatorial *trans*-positions within the bridging plane. The strong pseudo-Jahn–Teller effect of octahedral Mn(III) complexes is documented in a huge elongation of an octahedral axis, namely that including the long bridging Mn–F bond and the Mn–O bond. In spite of different charge of the anion in the fluoride phosphate, the octahedral geometry is almost the same as in the aqua-fluoro compounds. The strong distortion is reflected also in the ligand field spectra.

1. Introduction

Fluoromanganates(III) with d^4-high-spin configuration are well suited to study the influence of the structural topology on extent and direction of Jahn–Teller distortions [1]. It has been shown that small distortions, in some cases even averaged by a dynamical Jahn–Teller effect, are found in compounds with isolated anions like $[Co(H_2O)_6][MnF_6]$ [2]. The strongest distortions are encountered when the Jahn–Teller-active centers are strongly coupled, for instance in layer structures $AMnF_4$ (A = alkali metal, Tl), where in a square net of corner-sharing octahedra strongly asymmetrical bridges are formed ("antiferrodistortive ordering") [3–5]. This paper deals with some rare examples where two Jahn–Teller-active Mn(III) centers are coupled in dimers of edge-sharing $[MnF_5O]$ octahedra.

2. Results and discussion

2.1. Syntheses

$dabcoH_2[Mn_2F_8(H_2O)_2]\cdot 2H_2O$ (**1**) and $pipzH_2[Mn_2F_8(H_2O)_2]\cdot 2H_2O$ (**2**) crystallized from hydrofluoric acid solutions of manganese(III) acetate after adding an aqueous dabco or piperazine solution, respectively. $(dabcoH_2)_2[Mn_2F_8(H_2PO_4)_2]$ (**3**) formed from a hydrofluoric acid solution of $MnF_3\cdot 3H_2O$ after adding a solution of dabco in phosphoric acid. For details see Section 3.

2.2. Crystal structures

For all three compounds, the crystal structures could be determined by X-ray structure analyses on single crystals, the crystal data and experimental details of which are given in Section 3.

2.2.1. Compounds cat$[Mn_2F_8(H_2O)_2]\cdot 2H_2O$ (cat = $dabcoH_2$ (**1**), and $pipzH_2$ (**2**))

The structures are built from $dabcoH_2^{2+}$ or $pipzH_2^{2+}$ cations and $[Mn_2F_8(H_2O)_2]^{2-}$ anions that have not been reported before (Figs. 1a and 2). In similar systems, structures comprising isolated

* Corresponding author. Tel.: +49 6421 13197.
E-mail address: massa@chemie.uni-marburg.de (W. Massa).
[1] Present address: Am Oder-Spree-Kanal 12, 12527 Berlin, Germany.
[2] Present address: Dorfstr. 98, 07751 Milda, Germany.
[3] Present address: Leibniz-Institut für Katalyse e.V. an der Universität Rostock, Albert-Einstein-Str. 29a, 18059 Rostock, Germany.

0022-1139/$ – see front matter © 2011 Elsevier B.V. All rights reserved.
doi:10.1016/j.jfluchem.2011.05.023

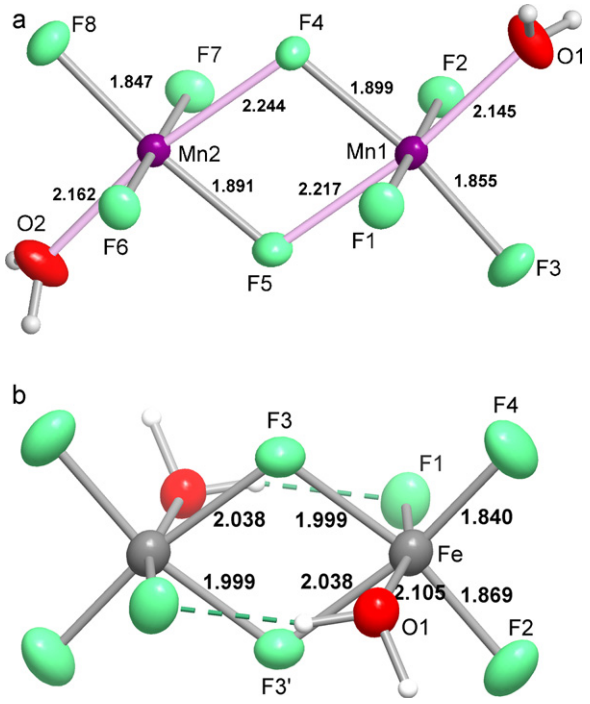

Fig. 1. (a) $[Mn_2F_8(H_2O)_2]^{2-}$ anion in (**1**) with selected bond lengths in Å (e.s.d.s 0.0017–0.0026). (b) $[Fe_2F_8(H_2O)_2]^{2-}$ anion in $[(CH_3)_4N][Fe_2F_8(H_2O)_2]$ [9] with selected bond lengths in Å (e.s.d.s 0.004–0.005). Displacement ellipsoids at the 50% probability level, H atoms as spheres with arbitrary radius, intramolecular H-bonds dashed.

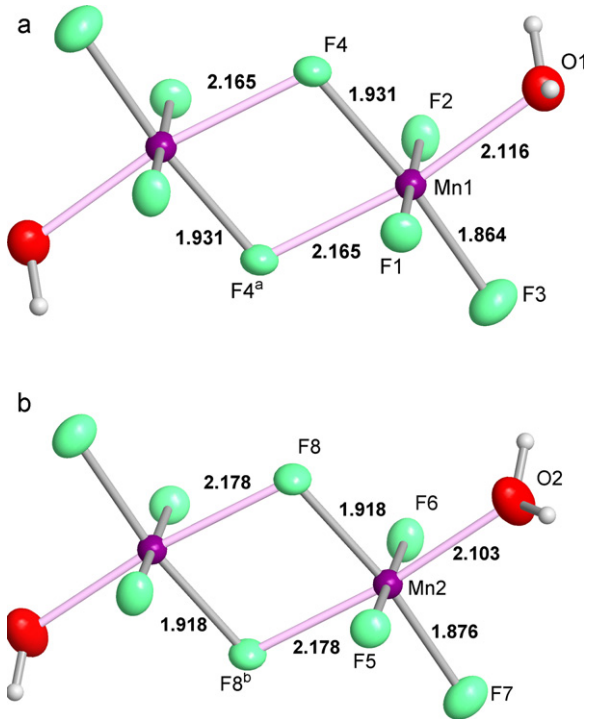

Fig. 2. (a and b) The two independent centrosymmetric anions in (**2**) with selected bond lengths in Å (e.s.d.s 0.0015–0.0020). Displacement ellipsoids at the 50% probability level, H atom as spheres with arbitrary radius.

anions such as $[MnF_5(H_2O)]^{2-}$ or $[MnF_5(H_2O)_2]^{-}$, or linear chains are observed (overview see [1]). In the dabco compound (**1**), the $[Mn_2F_8(H_2O)_2]^{2-}$ anion has no crystallographic symmetry but approaches point symmetry 2/m (C_{2h}). In the pipz compound (**2**), there are two independent centrosymmetrical anions, both with pseudosymmetry 2/m, too (Fig. 2). The anions can be described as dimers built from edge-sharing $[MnF_5(H_2O)]$ octahedra. The occurrence of double fluorine bridges is rare in the structural chemistry of fluorides [6–8] which is dominated by the connection of the octahedra via sharing of common vertices. Examples of dimeric anions of analogous composition were found in compounds $[(CH_3)_4N][M_2F_8(H_2O)_2]$ (M = Fe, Al) [9]. The respective Fe(III) compound is a very good reference structure for revealing the influence of the Jahn–Teller effect of Mn(III) because the ionic radius of Fe^{3+} is the same as that of Mn^{3+} (0.645 Å) [10] but the electronic configuration is highly symmetric d^5. In the iron compound, the position of the aqua ligands is *trans*-axial (Fig. 1b) while in both Mn(III) compounds it is *trans*-equatorial

Table 1
Bond lengths (Å) and selected angles (°) in the anions of $dabcoH_2[Mn_2F_8(H_2O)_2]\cdot 2H_2O$ (**1**), $pipzH_2[Mn_2F_8(H_2O)_2]\cdot 2H_2O$ (**2**), and $(dabcoH_2)_2[Mn_2F_8(H_2PO_4)_2]$ (**3**).

(**1**)		(**2**)		(**3**)	
Mn1–F1	1.824(2)	Mn1–F1	1.817(2)	Mn–F1	1.819(1)
Mn1–F2	1.812(2)	Mn1–F2	1.824(2)	Mn–F2	1.815(1)
Mn1–F3	1.855(2)	Mn1–F3	1.864(2)	Mn–F3	1.855(1)
Mn1–F4	1.899(2)	Mn1–F4	1.931(2)	Mn–F4	1.915(1)
Mn1–F5	2.217(2)	Mn1–F4^a	2.165(2)	Mn–F4^c	2.250(1)
Mn1–O1	2.145(3)	Mn1–O1	2.116(2)	Mn–O2	2.126(1)
Mn2–F6	1.835(2)	Mn2–F5	1.810(2)	P–O1	1.497(1)
Mn2–F7	1.805(2)	Mn2–F6	1.823(2)	P–O2	1.508(1)
Mn2–F8	1.847(2)	Mn2–F7	1.876(2)	P–O3	1.563(1)
Mn2–F5	1.891(2)	Mn2–F8	1.918(2)	P–O4	1.580(1)
Mn2–F4	2.244(2)	Mn2–F8^b	2.178(2)		
Mn2–O2	2.162(3)	Mn2–O2	2.103(2)		
F1–Mn1–F2	178.5(1)	F1–Mn1–F2	179.2(1)	F1–Mn–F2	177.49(5)
F3–Mn1–F4	170.8(1)	F3–Mn1–F4	173.9(1)	F3–Mn–F4	169.89(4)
F5–Mn1–O1	172.4(1)	F4^a–Mn1–O1	170.3(1)	F4^c–Mn–O2	164.14(4)
F6–Mn2–F7	178.5(1)	F5–Mn2–F6	179.7(1)		
F5–Mn2–F8	173.3(1)	F7–Mn2–F8	172.0(1)		
F4–Mn2–O2	170.3(1)	F8^b–Mn2–O2	173.4(1)		
F3–Mn1–O1	94.5(1)	F3–Mn1–O1	93.8(1)	F3–Mn–O2	102.25(5)
F4–Mn1–F5	77.7(1)	F4–Mn1–F4^a	78.0(1)	F4–Mn–F4^c	77.94(4)
F8–Mn2–O2	93.3(1)	F7–Mn2–O2	93.0(1)		
F4–Mn2–F5	77.2(1)	F8–Mn2–F8^b	78.5(1)		
Mn1–F4–Mn2	101.9(1)	Mn1–F4–Mn1^a	102.0(1)	Mn–F4–Mn^c	102.06(4)
Mn1–F5–Mn2	103.2(1)	Mn2–F8–Mn2^b	101.5(1)		

Symmetry-transformations: $^a 1-x, 1-y, 1-z$; $^b -x, 2-y, -z$; $^c -x, 1-y, -z$.

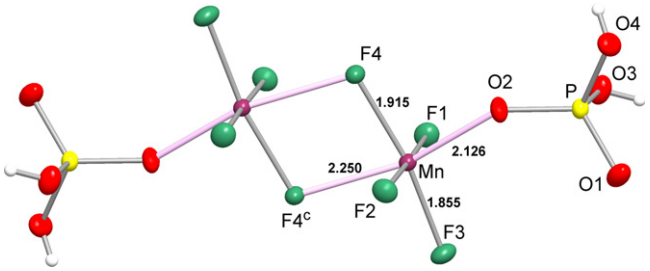

Fig. 3. $[Mn_2F_8(H_2PO_4)_2]^{4-}$ anion in (**3**) with selected bond lengths in Å (e.s.d.s 0.0009–0.0011). Displacement ellipsoids at the 50% probability level, H atoms as spheres with arbitrary radius.

(Figs. 1a and 2). Whereas the M–F–M bridges are rather symmetric in the Fe compound (Fe–F 1.999(4) and 2.038(5) Å) the M–F–M bridges in the Mn(III) structures show a strong asymmetry (Table 1). Obviously, the strong Pseudo-Jahn–Teller effect stabilizes the *trans*-equatorial positions of the aqua ligands because in this way an octahedral axis with two weak bonds – toward a bridging fluorine atom and a neutral aqua ligand – is formed providing optimum Jahn–Teller stabilization energy when this weak axis is additionally elongated. In the dimer of two elongated octahedra, the variant with asymmetrical bridges – thus parallel orientation of the long axes – is favored because in the alternative structure with symmetrical bridges (long/long and short/short) the Mn···Mn distance would become too short. Theoretical investigations based on DFT calculations and combined vibronic coupling and angular overlap analyses of various mixed-ligand Mn(III) fluorides including structures (**1**) and (**2**) [11] provide computational evidence for the observed experimental results though the strong influence of H-bonds in aqua-fluoro complexes prevents a satisfactory quantitative treatment.

Comparable double-bridged dimeric units with the same type of Jahn–Teller distortion in asymmetrical bridges have been found in $(pipzH_2)_3[Mn_4F_{18}(H_2O)]\cdot H_2O$ [12]. Here, two dimeric units $[F_4MnF_2MnF_4]$ and $[F_4MnF_2MnF_3(H_2O)]$ are corner-linked to form a tetrameric anion. A layer structure built from corner-sharing $[Mn_2F_8]$ dimers was found in $pipzH_2[Mn_2F_8]$ [13].

2.2.2. $(dabcoH_2)_2[Mn_2F_8(H_2PO_4)_2]$ (3)

A similar dimeric anion is found in (**3**), in which dihydrogenphosphate anions replace the *trans*-equatorial aqua ligands occurring in (**1**) and (**2**) (Fig. 3). The higher negative charge is compensated by an additional $dabcoH_2^{2+}$ cation per dimer. In spite of the different ligands and charge, the Jahn–Teller distorted geometry is rather similar to that of the aqua compounds (Table 1). Thus, the bond strengths of the Mn–OH_2 and the Mn–$OPO(OH)_2$ bonds seem to be quite similar. This is also confirmed by the observed comparable UV/vis spectra. Apart from some individual spread of bond lengths in structures (**1**)–(**3**), all these dimeric

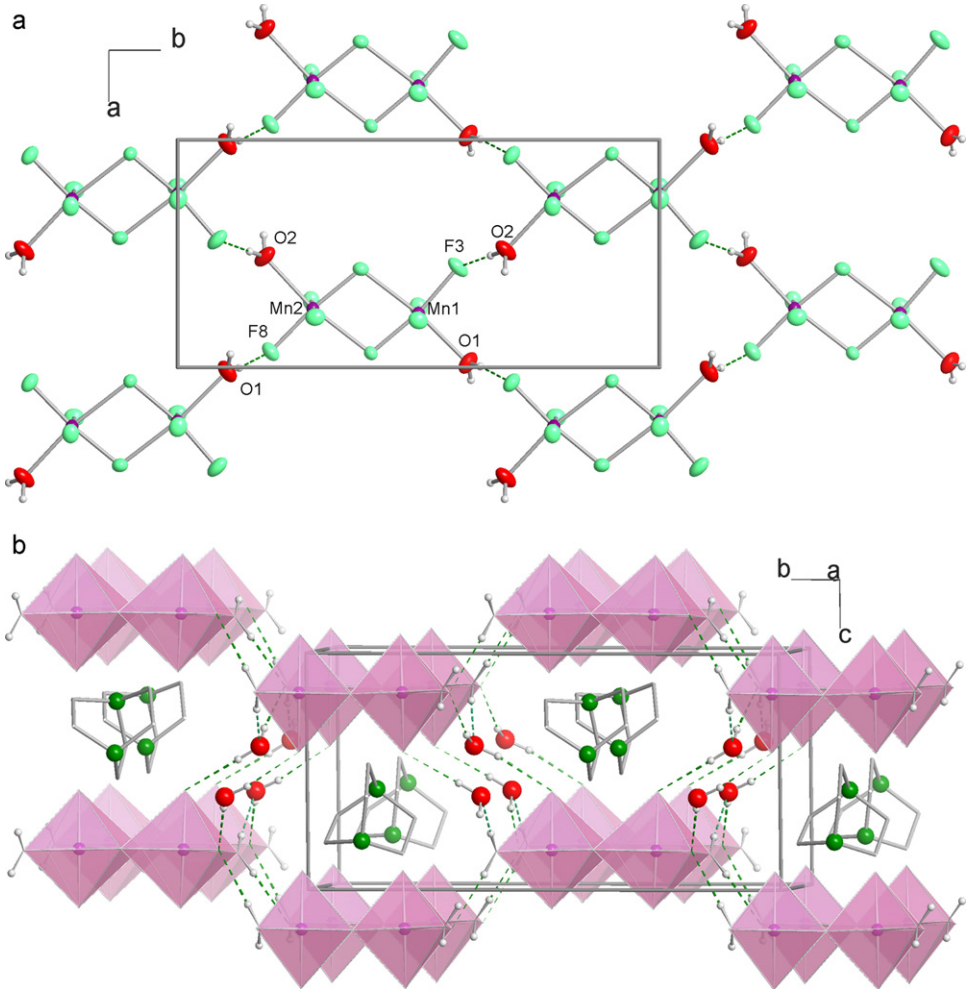

Fig. 4. (a) Linking of dimeric anions of structure (**1**) over strong O–H···F hydrogen bonds to layers in the *a*,*b*-plane. (b) View of structure (**1**) appr. along [1 0 0] showing the connection of the puckered anionic layers via water molecules resulting in channels along [1 0 0] filled by the $dabcoH_2$ cations. Dimeric anions as polyhedra, N black, O large bright, C medium, H small grey spheres.

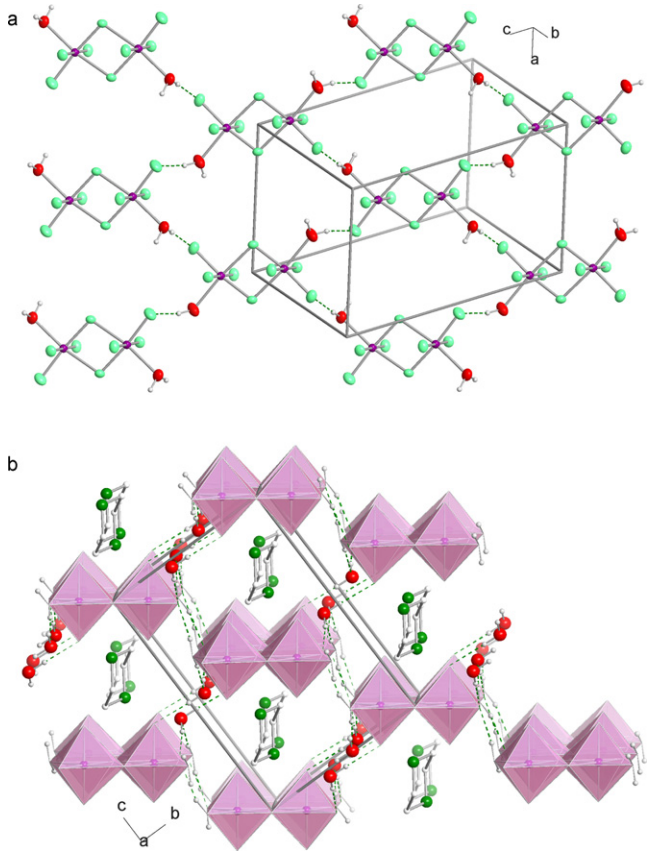

Fig. 5. (a) Layer of dimeric anions in (**2**) connected by strong O–H···F hydrogen bonds. View appr. from [0 2 1]. (b) View of structure (**2**) appr. along [1 0 0] showing the connection of the stair-like anionic layers via water molecules resulting in channels along [1 0 0] filled by the $pipzH_2$ cations. Dimeric anions as polyhedra, N black, O large bright, C medium, H small grey spheres.

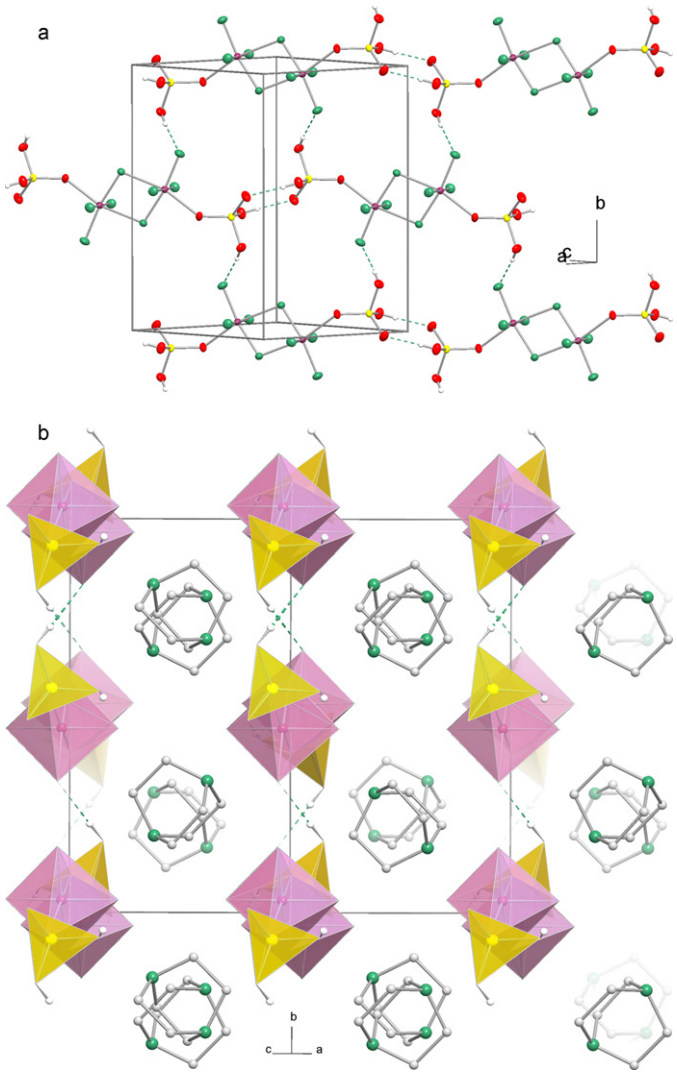

Fig. 6. (a) Anionic layer in structure (**3**) formed by strong hydrogen bonds O–H···F and O–H···O involving the dihydrogenphosphate ligands. Mn dark, F, P white, O grey, H small spheres. (b) Pseudo-tetragonal arrangement of chains of $dabcoH_2$ cations between the anionic layers of structure (**3**). Dimeric anions as grey polyhedra, phosphate as dark tetrahedra, N black, C medium, H small grey spheres.

anions belong to the most strongly distorted systems in the family of fluoromanganates(III), as documented also in the ligand field spectra (see Section 2.4, below).

2.2.3. Packing and hydrogen bonds

In all three structures, the dimeric anions are linked by hydrogen bonds to form layers. In (**1**) and (**2**), nets with meshes of four dimers are observed (Figs. 4a and 5a). In structure (**1**) the layers are oriented in the (0 0 1) plane and are puckered (Fig. 4b). In (**2**), stair-like layers are formed in the (0 1 1) plane (Fig. 5b). In both compounds, the hydrogen bonds are of the type O–H···F. In the fluoride phosphate (**3**), additional double hydrogen bonds O–H···O between dihydrogenphosphate groups provide meshes formed by three $[MnF_5O]$ octahedra and three phosphate tetrahedra (Fig. 6a). The resulting layers are parallel to the (1 0 $\bar{1}$) plane. The hydrogen bond geometries are summarized in Table 2.

As shown in Figs. 4b and 5b, the layers of (**1**) and (**2**) are interconnected via the non-coordinated water molecules by hydrogen bonds to form channels along the [1 0 0] directions that are occupied by the $dabcoH_2^{2+}$ or piperazinium(2+) cations, respectively.

In compound (**3**), the anionic layers (Fig. 6a) are stacked along [1 0 $\bar{1}$] leaving pseudotetragonal channels along [1 0 1] that contain the $dabcoH_2^{2+}$ cations (Fig. 6b).

The cations show in part larger anisotropy of the displacement ellipsoids indicating some dynamics or disorder. As the maximum displacement amplitudes were 0.29 Å (**1**), 0.21 Å (**2**), and 0.37 Å (**3**) only, no split-atom model was refined. The cations are tied to the anionic layers by weak N–H···F and N–H···O hydrogen bonds (Table 2).

2.3. Ligand field spectra

The UV/vis spectra recorded in reflection mode for the aqua-fluoromanganate(III) (**1**) and the phosphato-fluoromanganate(III) (**3**) are displayed in Fig. 7. The main transitions (in cm^{-1}), assigned according to [14], are: I ($^5B_{1g}$–$^5A_{1g}$) 14,500 (**1**), 14,100 (**3**); II ($^5B_{1g}$–$^5B_{2g}$) 18,300 (**1**), 18,000 (**3**); III ($^5B_{1g}$–^5E_g) 21,900 (**1**), 21,900 (**3**), the ligand field parameters (definition see [14]): Δ = 13,450 (**1**), 13,550 (**3**), $2\delta_1$ = 7250 (**1**), 7050 (**3**), δ_2 = 1200 (**1**), 1300 (**3**) cm^{-1}. The position of the first transition ($^5B_{1g}$–$^5A_{1g}$) related to the ground state splitting by the Jahn–Teller effect is slightly higher for the aqua-ligands (14,500 cm^{-1}) than for the phosphate ligands (14,100 cm^{-1}) but the ligand field parameter Δ is somewhat lower. Both parameters are in the upper range of energies found for fluoromanganates(III), close to that of $AMnF_4$ structures with antiferrodistortive ordering of $[MnF_6]$ octahedra in quadratic layers [14]. In this case a maximum of 15,500 cm^{-1} is observed for the first transition in $RbMnF_4$.

Table 2
Hydrogen bonds in structures (**1**) and (**2**). Distances in Å, angles in°, D = donor, A = acceptor.

D–H···A	*d*(D–H)	*d*(H···A)	*d*(D···A)	<(DHA)
(**1**)				
O1–H11···O3[a]	0.80	1.88	2.680(4)	172.8
O1–H12···F8[b]	0.80	1.96	2.756(3)	172.5
O2–H22···F3[c]	0.80	1.88	2.677(3)	176.4
O2–H21···O4	0.80	1.90	2.698(4)	171.2
O3–H31···F3	0.80	1.95	2.740(4)	170.0
O3–H32···F6[d]	0.80	1.96	2.759(4)	173.1
O4–H41···F8[e]	0.80	1.96	2.734(3)	162.2
O4–H42···F1[f]	0.80	1.97	2.764(4)	171.3
N1–H1···F6	0.91	2.05	2.802(3)	139.7
N1–H1···F1	0.91	2.47	3.093(3)	125.5
N1–H1···F5	0.91	2.53	3.217(2)	132.7
N2–H2···F2[g]	0.91	2.11	2.815(3)	133.4
N2–H2···F4[g]	0.91	2.17	2.912(2)	137.9
N2–H2···F7[g]	0.91	2.31	2.916(3)	123.5
Symmetry transformations used to generate equivalent atoms: [a] $x+1, y, z$, [b] $-x+2, y+1/2, -z+2$, [c] $-x+1, y-1/2, -z+2$, [d] $-x+1, y+1/2, -z+1$, [e] $x-1, y, z$, [f] $-x+1, y-1/2, -z+1$, [g] $x-1, y, z-1$.				
(**2**)				
O1–H1A···F8[a]	0.85	1.81	2.649(3)	166.3
O1–H1B···O4	0.85	1.91	2.747(3)	167.3
O2–H2A···O3	0.85	1.90	2.748(3)	176.8
O2–H2B···F4	0.85	2.01	2.825(3)	160.4
O2–H2B···F2	0.85	2.37	2.966(3)	128.3
O3–H3A···F7[b]	0.85	1.84	2.688(2)	174.0
O3–H3B···F8[c]	0.85	1.84	2.692(2)	175.9
O4–H4B···F3[c]	0.85	1.84	2.692(2)	176.2
O4–H4A···F4[a]	0.85	1.85	2.697(3)	171.7
N1–H1···F2	0.90	2.03	2.827(2)	146.9
N1–H1···F1	0.90	2.28	2.923(2)	127.7
N1–H1···F3[d]	0.90	2.42	2.912(2)	115.0
N1–H2···O4[d]	0.90	1.99	2.876(3)	168.7
N2–H4···F5[e]	0.90	1.98	2.787(2)	147.9
N2–H4···F6[e]	0.90	2.30	2.936(2)	127.8
N2–H4···F7[f]	0.90	2.46	2.975(2)	116.5
N2–H3···sO3[b]	0.90	1.96	2.856(3)	171.4

Symmetry transformations used to generate equivalent atoms: [a] $x+1, y, z$, [b] $-x+1, -y+1, -z$, [c] $-x+1, -y+2, -z+1$, [d] $-x+1, -y+1, -z+1$, [e] $x, y-1, z$, [f] $-x, -y+1, -z$.

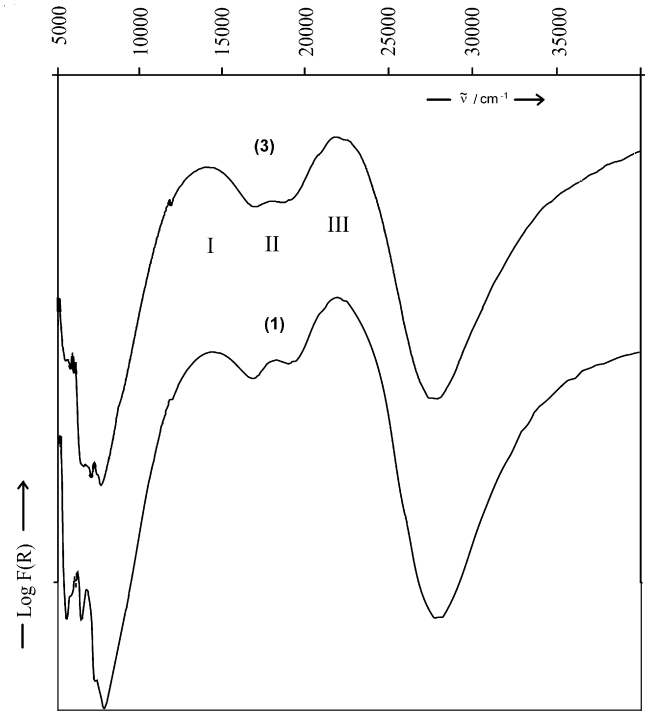

Fig. 7. UV/vis spectra of compounds (**1**) and (**3**) (*f*(*R*) = Kubelka–Munk function).

2.4. Conclusions

The double fluorine-bridged dimeric anions $[Mn_2F_8(H_2O)_2]^{2-}$ and $[Mn_2F_8(H_2PO_4)_2]^{4-}$ show remarkably strong Jahn–Teller distortion of the $[MnF_5O]$ coordination octahedra. The oxo ligands are in *trans*-equatorial position of the dimer, in contrast to *trans*-axial configuration of the analogous $[Fe_2F_8(H_2O)_2]^{2-}$ anion. This is attributed to stabilization by the strong pseudo Jahn–Teller effect. As usual in the structural chemistry of fluoromanganates(III), strong elongation of the octahedral axis bearing the weakest ligands is observed, here that with a bridging Mn–F bond and a $Mn–OH_2$ or $Mn–OPO(OH)_2$ bond. In the dimer of two elongated octahedra, parallel orientation of the long axes – resulting in very asymmetrical Mn–F–Mn bridges – is favored. The strong structural distortions correlate with extreme ligand field parameters.

3. Experimental

3.1. Syntheses

Crystals of $dabcoH_2[Mn_2F_8(H_2O)_2]\cdot 2H_2O$ (**1**) in form of brown columns were obtained from a solution containing 2.7 g (10 mmol) manganese(III) acetate dihydrate (Merck, for synthesis) in 30 mL 40% hydrofluoric acid after adding 10 mL of a 0.5 M solution of 1,4-diazabicyclo[2.2.2]octane (dabco, Merck, for synthesis) in H_2O.

Brown platelets of $pipzH_2[Mn_2F_8(H_2O)_2]\cdot 2H_2O$ (**2**) were precipitated from a solution of 2.7 g (10 mmol) manganese(III) acetate

Table 3
Crystallographic data, measuring and refinement conditions for the crystal structures of $dabcoH_2[Mn_2F_8(H_2O)_2]\cdot 2H_2O$ (**1**), $pipzH_2[Mn_2F_8(H_2O)_2]\cdot 2H_2O$ (**2**) and $(dabcoH_2)_2[Mn_2F_8(H_2PO_4)_2]$ (**3**).

	1	**2**	**3**
Crystal data			
Formula, M_r	$C_6H_{22}F_8Mn_2N_2O_4$, 448.14	$C_4H_{20}F_8Mn_2N_2O_4$, 422.10	$C_{12}H_{32}F_8Mn_2N_4O_8P_2$, 684.24
Crystal size (mm)	$0.12\times0.05\times0.03$	$0.50\times0.30\times0.07$	$0.30\times0.25\times0.20$
Color	Brown	Brown	Brown-green
Temperature (K)	293	293	203
Space group, Z	$P2_1$, $Z=2$	$P\bar{1}$, $Z=2$	$P2_1/n$, $Z=2$
Lattice constants (Å)			
a	6.944(1)	6.977(1)	9.3447(4)
b	14.689(3)	8.760(2)	12.5208(4)
c	7.307(1)	12.584(3)	9.7591(6)
Angles (°)			
α		83.79(3)	
β	93.75(3)	74.25(3)	94.392(8)
γ		71.20(3)	
Cell volume (Å^3)	743.7(2)	700.6(3)	1138.5(1)
Density d_c (g cm^{-3})	2.001	2.001	1.996
Absorption coefficient μ (mm^{-1})	1.803	1.907	1.356
Data collection			
Diffractometer	P4 (Siemens)	CAD4 (Enraf-Nonius)	CAD4 (Enraf-Nonius)
Radiation	MoK_α	MoK_α	MoK_α
Measuring range: max. θ (°)	30.00	29.00	29.94
Reflections (total)	2929	4009	3470
Completeness	99.7%	99.9%	99.8%
Refinement			
Reflections uniques/$>2\sigma(I)$	2398/2235	3722/2945	3300/2979
Parameters	217	197	204
wR_2 (all F^2)/R_1(obs. F)	0.0642/0.0240	0.1271/0.0451	0.0748/0.0280
Goodness of fit $S(F^2)$	1.026	1.062	1.060
Residual electron density max./min. (eÅ^{-3})	0.44/−0.31	0.92/−1.05	0.52/−0.55

dihydrate (Merck, for synthesis) in 30 mL 40% hydrofluoric acid after adding 5 mL of a 1 M aqueous solution of piperazine (Merck, waterfree, for synthesis).

For the synthesis of $(dabcoH_2)_2[Mn_2F_8(H_2PO_4)_2]$ (**3**), the following procedure arose from systematical investigations of the system Mn(III)/dabco/HF/H_3PO_4/H_2O varying concentrations and pH: Basic solution I: 16.6 g (100 mmol) $MnF_3\cdot 3H_2O$ (prepared from MnOOH as described in [15]) was dissolved in 10 M HF to obtain 50 ml solution. Basic solution II: 11.22 g dabco (97%, Acros Organics, 100 mmol) was dissolved in 2.2 ml 15 M H_3PO_4 (p.a., Merck) and filled up with H_2O to 100 ml. For reaction and crystallisation 1 ml of solution I and 4 ml of solution II were mixed, and 9 ml 10 M HF and 2.5 ml 15 M H_3PO_4 were added. Brown-green single crystals appeared when methanol was allowed to diffuse for 3 weeks over the gas phase to tubes containing 2 ml each of this mixture.

The compounds were characterised by single-crystal X-ray structure analyses.

3.2. Crystal structure analyses

The crystal data and experimental conditions for the structure determinations are collected in Table 3. For (**1**) and (**3**) absorption corrections via psi-scans were applied. The structures were solved by direct methods (SHELXS-86 [16]) and refined against all F^2 data using full matrix least squares methods (SHELXL-97) [17] using anisotropic displacement parameters for all heavier atoms. All hydrogen atoms could be localized from difference Fourier maps. For the cations in (**1**) and (**2**), they were kept riding on idealized positions with isotropic displacement parameters taken as 1.2 U_{eq} of their bonding partner. The water molecules were refined as rigid groups with isotropic displacement parameters of the H-atoms common per molecule. In (**3**), the better data allowed free refinement of the H atoms except that at C2, C4, and C6 of the $dabcoH_2$ cation. The latter C-atoms showed strongly elongated displacement ellipsoids indicating some rotational dynamics around the N···N axis. The attached H-atoms were kept riding on idealized positions, therefore, with displacement parameters taken as 1.2 U_{eq} of their bonding partners. All structure drawings were made with the DIAMOND program [18].

Crystallographic data (excluding structure factors) for the structures reported in this paper have been deposited with the Cambridge Crystallographic Data Center as supplementary publications no. CCDC-814885 (1), -814886 (2), and 814884 (3). Copies of the data can be obtained free of charge on application to CCDC, 12 Union Road, Cambridge CB2 1EZ, UK [Fax: int Code +44 1223 336 033; E mail: deposit@cam.ac.uk or via www.ccdc.cam.ac.uk/conts/retrieving.html].

3.3. UV/vis spectra

Spectra of (**1**) and (**3**) were recorded on powders at room temperature on a Hitachi U-3410 device in the range 5000–40,000 cm^{-1} using $BaSO_4$ as white standard. Before, powder diffractograms were recorded using CuK_a radiation which could be completely simulated by theoretical calculations based on the single crystal data.

Acknowledgement

The authors thank the Deutsche Forschungsgemeinschaft for financial support.

References

[1] W. Massa, Rev. Inorg. Chem. 19 (1999) 117.
[2] K. Wieghardt, H. Siebert, Z. Anorg, Allg. Chem. 381 (1971) 12–20.
[3] W. Massa, M. Steiner, J. Solid State Chem. 32 (1980) 137–143.
[4] M. Molinier, W. Massa, S. Khairoun, A. Tressaud, J.L. Soubeyroux, Z. Naturforsch. 46b (1991) 1669–1673.
[5] M. Molinier, W. Massa, Z. Naturforsch. 47b (1992) 783–788.
[6] D. Babel, A. Tressaud, in: P. Hagenmueller (Ed.), Inorganic Solid Fluorides, Academic Press, 1985, pp. 77–203.
[7] W. Massa, D. Babel, Chem. Rev. 88 (1988) 275–296.

[8] W. Massa, in: R.H. Crabtree (Ed.), Encyclopedia of Inorganic Chemistry, 2nd ed., Wiley & Sons, 2006, pp. 1535–1561.
[9] U. Bentrup, W. Massa, Z. Naturforsch. 46b (1991) 395–399.
[10] R.D. Shannon, Acta Cryst. A32 (1976) 751–767.
[11] D. Reinen, M. Atanasov, W. Massa, Z. Anorg, Allg. Chem. 632 (2006) 1375–1398.
[12] R. Stief, W. Massa, Z. Anorg, Allg. Chem. 630 (2004) 2502–2507.
[13] R. Stief, W. Massa, Z. Anorg, Allg. Chem. 632 (2006) 797–800.
[14] P. Köhler, W. Massa, D. Reinen, B. Hofmann, R. Hoppe, Z. Anorg, Allg. Chem. 446 (1978) 131–158.
[15] R. Stief, Ch. Frommen, J. Pebler, W. Massa, Z. Anorg, Allg. Chem. 624 (1998) 461–468.
[16] G.M. Sheldrick, SHELXS-86, Program for the Solution of Crystal Structures from Diffraction Data, Universität Göttingen, 1986.
[17] G.M. Sheldrick, SHELXL-97, Program for the Refinement of Crystal Structures, Universität Göttingen, 1997.
[18] K. Brandenburg, DIAMOND 3.2e, Crystal Impact GbR, Bonn, 2010.